Microfluid Nanofluid (2015) 18:57–64
DOI 10.1007/s10404-014-1405-z

RESEARCH PAPER

Capillary filling speed of ferrofluid in hydrophilic microscope slide nanochannels

Ju-Nan Kuo · Wei-Kai Wang

Received: 13 January 2014 / Accepted: 17 April 2014 / Published online: 7 May 2014

Abstract The capillary filling speed of ferrofluid in hydrophilic nanofluidic channels is investigated under various temperature and constant magnetic field conditions. Nanochannels with depths ranging from 50 to 150 nm and widths of 30 to 200 μm are fabricated on borosilicate glass substrates using buffered oxide wet etching and glass–glass fusion bonding techniques. The capillary filling speed of the ferrofluid is measured experimentally and compared with the theoretical results predicted by the classical Washburn equation. It is found that the experimental filling speed is significantly slower than the theoretical filling speed due to the erroneous assumption in the Washburn model of a constant contact angle irrespective of the flow rate and the presence of flow obstructions. The experimental results show that the filling speed reduces with a reducing channel depth, an increasing ferrofluid concentration, a lower operating temperature and an increased filling length. However, the filling speed is enhanced in the presence of an external magnetic field.

Keywords Capillary filling · Ferrofluid · Glass substrate · Hydrophilic · Nanochannels

1 Introduction

Capillary action is ubiquitous in nature and is exploited and harnessed for affecting the transport of liquids in a vast number of natural and manmade systems. For example, capillary forces make possible the patterned transfer of arrays of solutions via the contact of pins with a biochip carrier (Schena et al. 1995). Capillary action is particularly pronounced in nanochannels due to the large surface-to-volume ratio in the nanoscale regime. As a result, capillary action provides an effective means of simplifying the design of nanofluidic systems since it eliminates the need for additional accessories such as syringe pumps or electrical/centrifugal driving devices (Tas et al. 2004; Lai et al. 2004; Eijkel and van den Berg 2006). However, in most cases, the capillary flow rate is lower than that predicted in theory as the channel dimension reduces to the nanoscale and beyond (Jung et al. 2009; Hamblin et al. 2011). This phenomenon has been variously attributed to electroviscosity effects (Mortensen and Kristensen 2008; Haneveld et al. 2008) and variations in the dynamic contact angle (Zhu and Petkovic-Duran 2010). However, while the exact mechanism responsible for the diminution of the flow rate may not be fully understood, previous studies have shown that the physical behavior of fluids in the nanoscale regime is markedly different from that observed in microscale structures (Turner et al. 2002). Consequently, in developing high-performance nanofluidic devices, a detailed understanding of the dynamic filling behavior of fluids at the nanoscale is required.

Recent developments in the nanotechnology field now make possible the fabrication of nanofluidic devices, in which the channels have at least one characteristic dimension less than 100 nm (Eijkel and Van Den Berg 2005; Perry and Kandlikar 2006; Xia et al. 2012; Duan et al. 2013). Such devices not only have many practical applications, including DNA analysis and the selective trapping and concentration of nanoparticles and viruses

J.-N. Kuo (✉) · W.-K. Wang
Department of Automation Engineering, National Formosa University, No. 64, Wenhua Rd., Huwei, Yunlin 632, Taiwan
e-mail: junan@nfu.edu.tw

W.-K. Wang
e-mail: hashopig@hotmail.com

(Hamblin et al. 2010) but also enable the experimental exploration of the unique fluid flow properties observed as the characteristic channel size approaches the molecular scaling length (Thamdrup et al. 2007; Abgrall and Nguyen 2008). Nanofluidic devices are generally fabricated on silicon substrates since the resulting nanochannels have an inherent hydrophilic property (Han and Craighead 2000; Hoang et al. 2009) and are therefore conducive to fluid flow. However, silicon-based devices have poor biocompatibility and require the use of complicated and expensive fabrication processes (Haneveld et al. 2003). As a result, they have only limited real-world applicability.

Ferrofluids are synthetic compounds comprising colloidal suspensions of single-domain magnetic nanoparticles in a carrier liquid (Popplewell and Rosensweig 1996). Due to their magnetic properties, ferrofluids can be easily manipulated via the application of a time-varying external magnetic field. Many studies have demonstrated the feasibility of using a ferrofluidic plug to pump a secondary, immiscible, nonmagnetic liquid (Hartshorne et al. 2004; Yamahata et al. 2005; Sun et al. 2007). As a result, the magnetic actuation of ferrofluids has attracted increasing interest in many fields, including biomedicine (Al-Halhouli et al. 2010), microelectronics (Jin and Aluru 2011), biological microelectromechanical systems (bioMEMS) (Chen et al. 2011). However, studies on the capillary flow of ferrofluids in nanochannels with characteristic dimensions ranging from several to hundreds of nanometers are still at an early stage.

The micro-/nanochips used in ferrofluidic applications are generally fabricated on polymethyl-methacrylate (PMMA) or silicon substrates. However, both materials have poor manufacturability and low biocompatibility. Accordingly, in the present study, nanochannels with depths ranging from 50 to 150 nm and widths ranging from 30 to 200 μm are fabricated on borosilicate glass substrates. The proposed fabrication method results in a high device yield, a low fabrication cost and fast capillary-driven flow. It is intrinsically hydrophilic, which could allow pumpless feeding of a biological sample. The nanochannels are then used to perform a series of investigations into the capillary filling speed of ferrofluid under various temperature and constant magnetic field conditions. The experimental results are compared with the theoretical results, and the difference between them is analyzed and discussed. These experiments are of practical value, because nanofluidic channels are usually filled by capillary action, and currently no accurate data are available about the filling speed of ferrofluid. They are of fundamental importance because they may reveal whether the dynamics of ferrofluid in nanoconfinement deviates from its bulk value.

2 Experimental method

The nanochannels fabricated in the present study were designed using AutoCAD software and then transferred to a plastic photomask. The mask contained an array of three parallel lines, each with a length of 8 mm and width ranging from 30 to 200 μm and each spaced at a distance of 500 μm from its neighbors. The nanofluidic channels were fabricated on borosilicate glass slides with a thickness of 1.1 mm. The details of the fabrication process and the characterization of the resulting channels are presented in a previous study by the present group (Kuo and Lin 2012a). However, briefly, the substrates were coated with a thin layer of photoresist and then exposed using UV light through the photomask. The patterned substrates were immersed in a 0.5 % diluted buffered oxide etchant (BOE 6:1) at room temperature. The required nanochannel depth (50–150 nm) was then achieved by carefully controlling the etching time. Following the etching process, the remaining photoresist was stripped from the substrate surface in an acetone solution, and the substrate was then dipped in a 1 M HCl solution for 2 min in order to remove any precipitated particles and to improve the surface flatness. The substrate was then cleaned with piranha solution. (Note that the piranha solution used is not only to clean the substrate, but also to increase its hydrophilicity.) Finally, the glass substrate and an unpatterned borosilicate slide were heated in a furnace at 400 °C for 8 h and then sealed using a thermal fusion bonding process performed at a temperature of 580 °C for a further 8 h.

Figure 1 shows the variation of the channel depth with the etching time. It is seen that the etching rate is approximately 10.1 nm/min. It is noted that this etching rate is

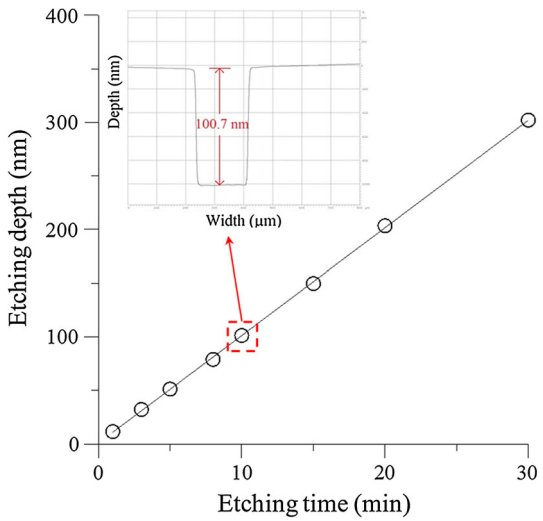

Fig. 1 Variation of etched channel depth with etching time. *Inset* shows profile measurement of nanochannel with depth of 100.7 nm

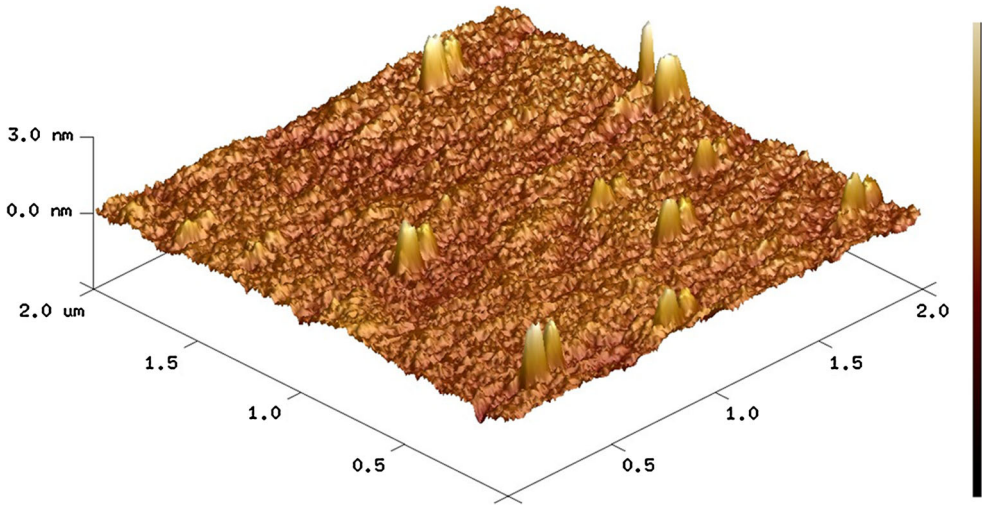

Fig. 2 AFM image of surface profile of glass channel etched in BOE and cleaned in 1 M HCl and piranha solution

much lower than that reported by Mao and Han for glass substrates (24 nm/min) (Mao and Han 2005). The difference between the two etching rates is due to a diluted buffered oxide etchant. The surface profiles of the etched nanochannels were measured using a surface profilometer (Dektak 6 M, Veeco). The inset in Fig. 1 shows the typical results obtained for a channel with a depth of 100.7 nm (etching time: 10 min). It is observed that the etching process results in a relatively smooth and well-defined nanochannel. Having etched the glass slides, they were immersed in 1 M HCl solution for 2 min in order to remove any precipitated particles and to further enhance the surface flatness. Figure 2 shows the surface profile of a substrate etched for 10 min as measured by an atomic force microscope (AFM, DI-3100, Veeco). From inspection, the average surface roughness (Ra) within the scanned area (2.0×2.0 μm^2) is found to be approximately 0.143 nm, while the maximum peak-to-peak height (Rmax) is 3.01 nm. Figure 3 presents a cross-sectional scanning electron microscope (SEM) image of a bonded nanochannel with a depth of 150 nm. It is seen that the etched channel is completely open (i.e., contains no obstacles) and has a uniform cross-section. In addition, no obvious interface is observed between the upper and lower slides. Therefore, the effectiveness of the glass–glass bonding process is confirmed.

The nanofluidic chip fabricated in the present study incorporated three parallel nanochannels with a length of 8 mm, depths of 50, 100 and 150 nm and widths of 30, 100 and 200 μm, respectively. The capillary flow experiments were performed using a commercially available ferrofluid (USPIO-101, TANBead) comprising Fe_3O_4 magnetite particles with an average diameter of 6.2 nm suspended in an aqueous medium. According to the manufacturer's specification, the room temperature (25 °C) properties of the ferrofluid were as follows: particle density 5.4 g/cm^3,

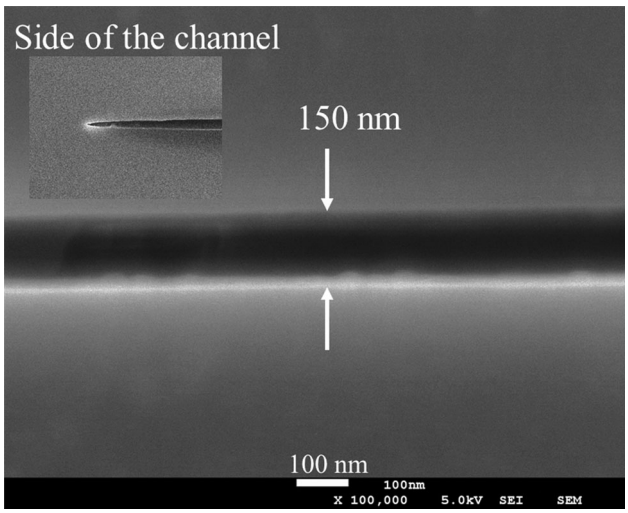

Fig. 3 Cross-sectional SEM image of nanochannel with depth of 150 nm

saturation magnetization 7 emu/g and viscosity 0.005 Ns/m^2. The filling experiments were performed using three ferrofluid concentrations, namely 0.1, 1 and 10 mg/ml, respectively. Figure 4 presents a schematic illustration of the nanofluidic chip and the capillary filling operation. As shown, a drop of ferrofluid was placed at the entry of each nanochannel using a pipette, and the nanofluidic chip was placed horizontally. The fluid was drawn into the nanochannel under the effects of capillary action and then flowed through the channel until it reached the exit. The change in position of the moving meniscus was recorded over time at a rate of 30 frames per second using a charge-coupled device (CCD) camera attached to a microscope. The filling rate of the ferrofluid was investigated under three different temperature conditions (i.e., 4, 25 and 50 °C) and with and without the presence of an external magnetic field, respectively.

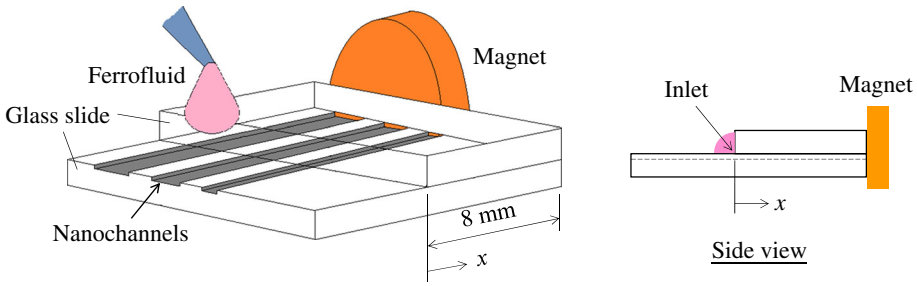

Fig. 4 Schematic illustration of nanofluidic chip used in ferrofluid filling experiments

The capillary filling speed in a rectangular channel can be described theoretically by the classical Washburn model (Washburn 1921), which takes into account both the capillary force sucking the liquid into the channel and the viscous drag force which opposes its motion. In accordance with this model, the position of the moving meniscus x as a function of time t can be obtained as (Tas et al. 2004)

$$x = \sqrt{\frac{\gamma \cos(\theta) h t}{3\mu}}, \tag{1}$$

where γ is the surface tension of the liquid in air, θ is the contact angle of the liquid on the channel walls, h is the channel height and μ is the viscosity of the liquid.

3 Results and discussion

Microscope slide/coverslip channels are typically hydrophilic with a contact angle for water of round 60° (Kuo and Lin 2012b). As a result, capillary action is rather suppressed. Accordingly, the present nanofluidic channels were cleaned with piranha solution in order to render them more hydrophilic, and thus more amenable to capillary flows. The hydrophilicity of the treated nanofluidic channels was evaluated by measuring the advancing contact angles of DI water and ferrofluids with concentrations ranging from 0.1 to 10 mg/ml, respectively, on a flat glass slide using a contact angle analyzer (FTA 188, First Ten Angstroms). The corresponding results are shown in Fig. 5. It is seen that the contact angle of the various liquids ranges from approximately 32–34°. In other words, the cleaning process results in a significant improvement in the hydrophilicity of the glass substrate. In practice, the contact angle of a moving liquid in a channel is not constant, but depends on the wetting-line velocity, which varies in turn with the instantaneous force balance that prevails during capillary filling. However, the classical Washburn model given in Eq. (1) assumes the contact angle to be constant and independent of the flow rate in a continuously flowing stream of liquid.

Figure 6 shows the variation of the capillary meniscus position with the square root of the filling time in nanochannels with a depth of 150 nm and widths of 30, 100 and 200 μm, respectively. Note that the ferrofluid concentration is 10 mg/ml in every case. It is seen that a

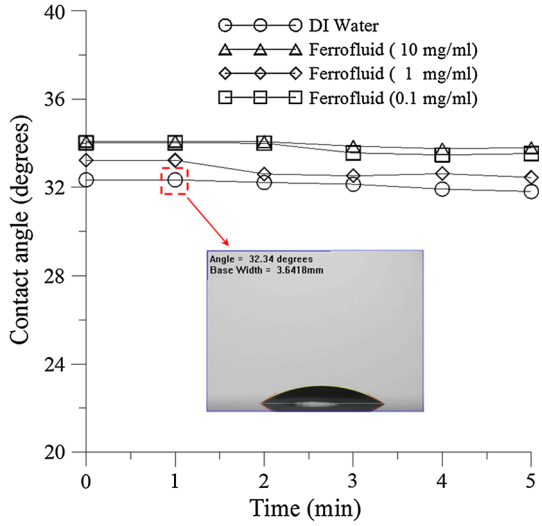

Fig. 5 Measured variation of contact angle of DI water and ferrofluids on cleaned flat glass surface

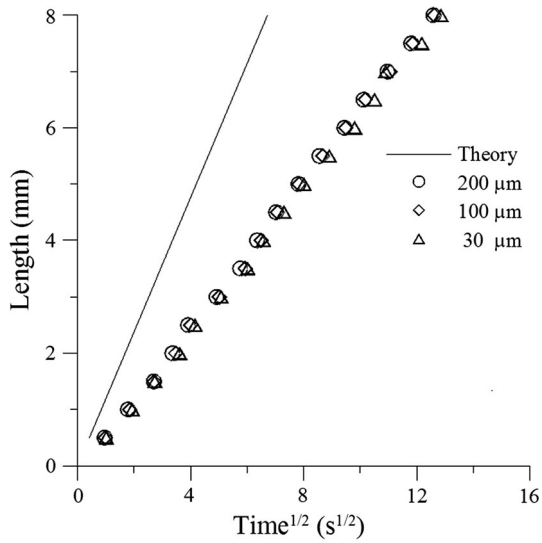

Fig. 6 Variation of meniscus position with square root of filling time. Note that theoretical results obtained using Eq. (1) are also presented for comparison purposes

near perfect linear relationship exists between the meniscus position and the filling time. In addition, it is observed that the flow rate is insensitive to the channel width. It can be seen that the experimental flow rate is notably lower than that predicted using Eq. (1). This result is reasonable since, as discussed above, the Washburn model assumes the contact angle to have a constant value, whereas in practice the contact angle actually depends on the instantaneous force balance which prevails during the capillary filling process, and for nanochannels this value has been shown to be larger than expected (Zhu and Petkovic-Duran 2010; Hamblin et al. 2011). Therefore, the experimental meniscus position (or speed) is lower than that predicted using Eq. (1). Furthermore, in nanoscale channels, the fluid flow is opposed not only by the viscous drag force but also by the effects of surface conduction and double-layer overlap (Eijkel et al. 2004). As a result, the Washburn model understates the contact angle, and therefore overestimates the meniscus position at any point during the filling process.

Figure 7a shows the measured position of the capillary meniscus as a function of the square root of the filling time for nanochannels with a width of 30 μm and depths of 50, 100 and 150 nm, respectively. It is seen that the meniscus position is linearly related to the square root of the filling time. In addition, it is observed that the flow rate reduces with a reducing channel depth. These curves are linear ($x^2 \propto t$, i.e., the meniscus position squared proportional to the filling time), and the taller channels fill much more quickly than the shorter channels ($x^2/t \propto h$, i.e., the flow rate proportional to the channel depth), as predicted by the Washburn equation. The reduction in the flow rate with a reducing channel depth is further illustrated in Fig. 7b. (Note that the nanochannel again has a width of 30 μm.). From inspection, the average flow rate is found to be 0.094, 0.069 and 0.032 mm/s for channel depths of 150, 100 and 50 nm, respectively. (Note that the average velocity is computed over the total length of the channel (i.e., 8 mm) in every case.) In addition, it is seen that for all values of the channel depth, the flow velocity reduces with an increasing filling length as a result of the corresponding increase in the viscous drag force.

The effect of the ferrofluid concentration on the capillary filling speed was evaluated by performing filling experiments using ferrofluids with concentrations of 0.1, 1 and 1.0 mg/ml, respectively. Figure 8 presents the experimental results obtained for the variation of the meniscus position with the flow velocity as a function of the ferrofluid concentration. (Note that the nanochannel has a width of 200 μm and a depth of 150 nm in every case.) It is seen that for all three ferrofluid concentrations, the filling speed reduces significantly as the filling length increases. Moreover, it is observed that the flow velocity also reduces with an

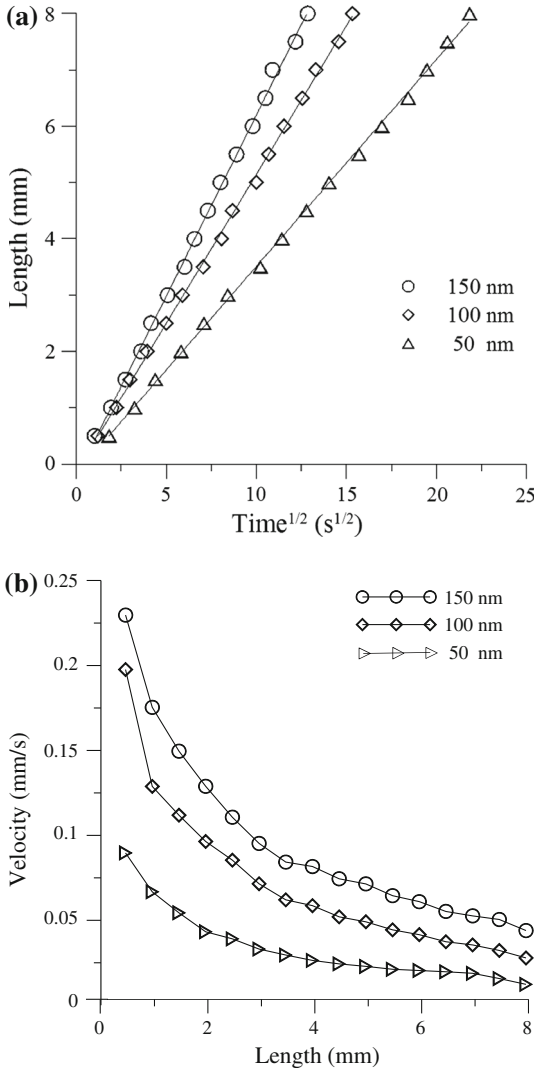

Fig. 7 **a** Variation of meniscus position with filling time as function of channel depth, and **b** variation of meniscus position with flow velocity as function of channel depth

increasing ferrofluid concentration. From inspection, the average flow velocities of the ferrofluids with concentrations of 0.1, 1 and 10 mg/ml are found to be 0.601, 0.453 and 0.111 mm/s, respectively. (Note that the average flow rate is calculated over the total channel length in every case.) It is noted that the present results are consistent with the finding in a previous study (Saha et al. 2009) that the capillary flow rate in microchannels is significantly dependent on the surface tension and viscosity of the fluid.

The operating temperature has a critical effect on the viscosity and flow rate of ferrofluids (Saha et al. 2009). Accordingly, a series of filling experiments were performed under operating temperatures of 4, 25 and 50 °C, respectively, using a ferrofluid sample with a concentration of 10 mg/ml and a nanochannel with a width of 200 μm and a depth of 150 nm. In performing the filling experiments at

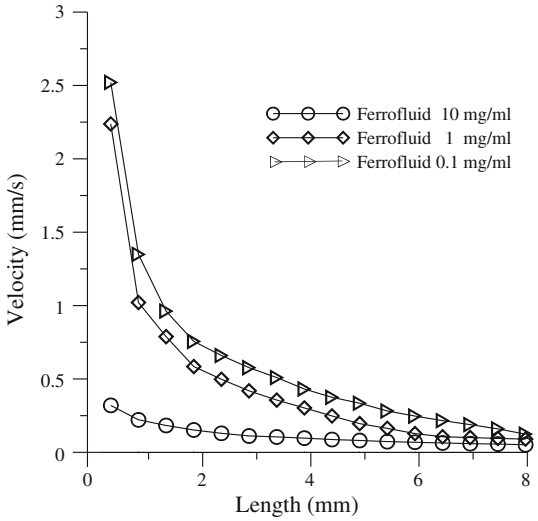

Fig. 8 Variation of meniscus position with flow velocity for ferrofluids with concentrations ranging from 0.1 to 10 mg/ml

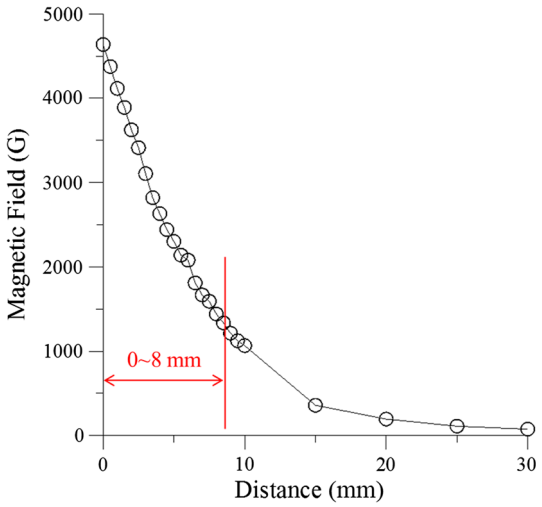

Fig. 10 Variation of magnetic field strength with distance from magnet

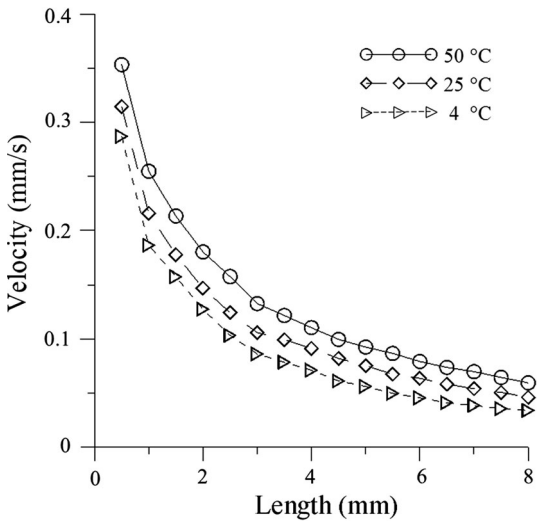

Fig. 9 Variation of meniscus position with flow velocity as function of operating temperature

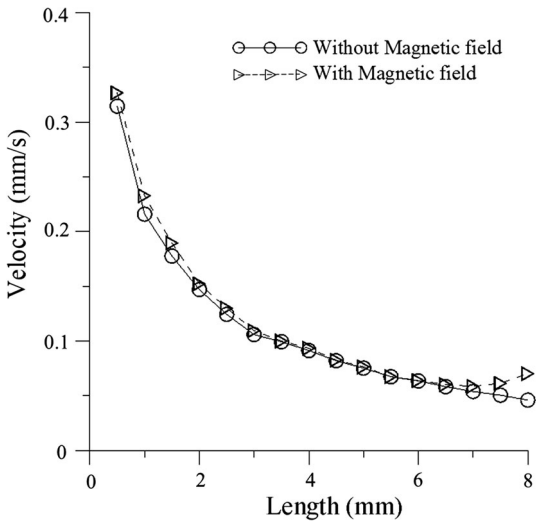

Fig. 11 Variation of meniscus position with flow velocity with and without magnetic field, respectively

temperatures of 4 and 50 °C, the ferrofluid sample and the chip were cooled in a fridge and heated in an oven, respectively. The corresponding experimental results are presented in Fig. 9. As expected, the flow velocity increases with an increasing temperature due to the corresponding reduction in the viscosity. From inspection, the average flow velocities are found to be 0.091, 0.111 and 0.134 mm/s for operating temperatures of 4, 25 and 50 °C, respectively.

Finally, a series of experimental trials were conducted to examine the effects of an external magnetic field on the capillary filling speed. Firstly, a magnetometer (MG-3002, Lutron) was used to determine the variation of the magnetic field intensity within the nanochannel as a function of the distance from the magnet (Note that the magnet was placed at the exit of the microchannel, see Fig. 4). As shown in Fig. 10, the magnetic field intensity reduces nonlinearly with an increasing distance. Specifically, the intensity reduces rapidly with an increasing distance for the range of 0–20 mm, but then decreases more slowly thereafter. The effect of the magnetic field on the filling speed was investigated using a ferrofluid sample with a concentration of 10 mg/ml and a nanochannel with a width of 200 μm and a depth of 150 nm. The results presented in Fig. 11 show that the flow velocity reduces dramatically with an increasing filling length. However, toward the exit of the nanochannel, the flow velocity suddenly increases due to the presence of the magnetic field. The average flow velocity is found to have values of 0.117 and 0.111 mm/s with and without the magnetic field, respectively. Since the

limited cross-sectional area of the nanochannels can only provide a small sample volume, which made the effect of an external magnetic field was weakened. The two curves in this figure represent an average four times individual channel filling experiments were obtained, where the average flow velocity uncertainly is 3.5 %. Comparing the results presented in Fig. 11 with those presented in Fig. 8 for the ferrofluid with a concentration of 10 mg/ml, it is seen that the application of an external magnetic field is beneficial in compensating for the lower flow rate associated with a ferrofluid of a higher concentration. In addition, compared with Fig. 8, it is observed that the flow rate reduces with an increasing concentration due to the greater viscosity, but an increasing concentration also increases the attractive effect of the magnetic field, particularly toward the end of the channel.

4 Conclusions

This study has performed an experimental investigation into the capillary filling speed of ferrofluids in glass-based nanofluidic channels under various temperature and constant magnetic field conditions. The results have shown that the theoretical predictions for the filling speed obtained using the classical Washburn model are higher than the experimental values due to the erroneous assumption of a constant contact angle for all values of the flow rate and the presence of microscopic flow obstructions. In addition, it has been shown that the capillary filling speed reduces with a reducing nanochannel depth, an increasing ferrofluid concentration, a reducing operating temperature and an increasing filling length. Moreover, the filling speed increases under the effects of an external magnetic field. Overall, the results presented in this study suggest that glass-based nanochannels have hydrophilic surface for use in a wide variety of pumpless liquid transport applications.

Acknowledgments The authors gratefully acknowledge the financial support provided to this study by the National Science Council of Taiwan under Grant No. NSC 101-2221-E-150-036. In addition, the access provided to fabrication equipment by the Common Lab for Micro/Nano Science and Technology of National Formosa University is also greatly appreciated.

References

Abgrall P, Nguyen NT (2008) Nanofluidic devices and their applications. Anal Chem 80(7):2326–2341

Al-Halhouli AT, Kilani MI, Buttgenbach S (2010) Development of a novel electromagnetic pump for biomedical applications. Sens Actuators A 162:172–176

Chen H, Abolmatty A, Faghri M (2011) Microfluidic inverse phase ELISA via manipulation of magnetic beads. Microfluid Nanofluid 10:593–605

Duan C, Wang W, Xie Q (2013) Review article: fabrication of nanofluidic devices. Biomicrofluidics 7:026501

Eijkel JCT, van den Berg A (2005) Nanofluidics: What is it and what can we expect from it? Microfluid Nanofluid 1(3):249–267

Eijkel JCT, van den Berg A (2006) The use of capillarity for passive flow handling in lab on a chip devices. Lab Chip 6(11): 1405–1408

Eijkel JCT, Bomer J, Tas NR, van den Berg A (2004) 1-D nanochannels fabricated in polyimide. Lab Chip 4:161–163

Hamblin MN, Xuan J, Maynes D, Tolley HD, Belnap DM, Woolley AT, Lee ML, Hawkins AR (2010) Selective trapping and concentration of nanoparticles and viruses in dual-height nanofluidic channels. Lab Chip 10:173–178

Hamblin MN, Hawkins AR, Murray D, Maynes D, Lee ML, Woolley AT, Tolley HD (2011) Capillary flow in sacrificially etched nanochannels. Biomicrofluidics 5:021103

Han J, Craighead HG (2000) Separation of long DNA molecules in a microfabricated entropic trap array. Science 288:1026–1029

Haneveld J, Jansen H, Berenschot E, Tas N, Elwenspoek M (2003) Wet anisotropic etching for fluidic 1D nanochannels. J Micromech Microeng 13:S62–S66

Haneveld J, Tas NR, Brunets N, Jansen HV, Elwenspoek M (2008) Capillary filling of sub-10 nm nanochannels. J Appl Phys 104:014309

Hartshorne H, Backhouse CJ, Lee WE (2004) Ferrofluid-based microchip pump and valve. Sensor Actuators B Chem 99:592–600

Hoang HT, Nolten IMS, Berenschot JW, Boer MJD, Tas NR, Haneveld J, Elwenspoek MC (2009) Fabrication and interfacing of nanochannel devices for single-molecule studies. J Micromech Microeng 19:065017

Jin X, Aluru NR (2011) Gated transport in nanofluidic devices. Microfluid Nanofluid 11:297–306

Jung MO, Telli F, de Sissi B, Frieder M (2009) Capillarity-driven dynamics of water-alcohol mixtures in nanofluidic channels. Microfluid Nanofluid 9:123–129

Kuo JN, Lin YK (2012a) Fabrication of 20 nm shallow nanofluidic channels using coverslip thin glass–glass fusion bonding method. Jpn J Appl Phys 51:095202

Kuo JN, Lin YK (2012b) Capillary-driven dynamics of water in hydrophilic microscope coverslip nanochannels. Jpn J Appl Phys 51:105201

Lai SY, Wang SN, Luo J, Lee LJ, Yang ST, Madou MJ (2004) Design of a compact disk-like microfluidic platform for enzyme-linked immunosorbent assay. Anal Chem 76:1832–1837

Mao P, Han J (2005) Fabrication and characterization of 20 nm planar nanofluidic channels by glass–glass and glass–silicon bonding. Lab Chip 5:837–844

Mortensen NA, Kristensen A (2008) Electroviscous effects in capillary filling of nanochannels. Appl Phys Lett 92:063110

Perry JL, Kandlikar SG (2006) Review of fabrication of nanochannels for single phase liquid flow. Microfluid Nanofluid 2(3):185–193

Popplewell J, Rosensweig RE (1996) Magnetorheological fluid composites. J Phys D Appl Phys 29(9):2297–2303

Saha AA, Mitra SK, Tweedie M, Roy S, McLaughlin J (2009) Experimental and numerical investigation of capillary flow in SU8 and PDMS microchannels with integrated pillars. Microfluid Nanofluid 7:451–465

Schena M, Shalon D, David RW, Brown PO (1995) Quantitative monitoring of gene expression patterns with a complementary DNA microarray. Science 270:467–470

Sun Y, Kwok YC, Nguyen NT (2007) A circular ferrofluid driven microchip for rapid polymerase chain reaction. Lab Chip 7:1012–1017

Tas NR, Haneveld J, Jansen HV, Elwenspoek M, van den Berg A (2004) Capillary filling speed of water in nanochannels. Appl Phys Lett 85:3274–3276

Thamdrup LH, Persson F, Bruus H, Kristensen A, Flyvbjerg H (2007) Experimental investigation of bubble formation during capillary filling of SiO_2 nanoslits. Appl Phys Lett 91:163505

Turner SWP, Cabodi M, Craighead HG (2002) Confinement-induced entropic recoil of single DNA molecules in a nanofluidic structure. Phys Rev Lett 88:128103

Washburn EW (1921) The dynamics of capillary flow. Phys Rev 17:273–283

Xia D, Yan J, Hou S (2012) Fabrication of nanofluidic biochips with nanochannels for applications in DNA analysis. Small 8(18): 2787–2801

Yamahata C, Chastellain M, Parashar VK, Petri A, Hofmann H, Gijs MAM (2005) Plastic micropump with ferrofluidic actuation. J Microelectromech Syst 14:96–102

Zhu Y, Petkovic-Duran K (2010) Capillary flow in microchannels. Microfluid Nanofluid 8:275–282